

A Directional and Latitude Survey of Cosmic Rays at High Altitudes*

J. R. WINCKLER,** T. STIX, K. DWIGHT, AND R. SABIN
Palmer Physical Laboratory, Princeton University, Princeton, New Jersey

(Received April 4, 1950)

The directional distribution of cosmic rays at atmospheric depths of 15 to 25 g/cm² has been measured with large counter telescopes carried by constant-level plastic balloons at geomagnetic latitudes of 0°, 20°, 30°, and 40°. From the vertical flux measurements an energy spectrum for primary protons is obtained which has the form $N(E)=0.27/E^{1.9}$, where $N(E)$ is the number of particles in unit energy range at the energy E . The corresponding formula for primaries consisting entirely of alpha-particles is $N(E)=0.32/E^{1.81}$. The power law can be fitted between about 1 and 14 Bev, but there is good evidence that the spectrum flattens out below 1 Bev and becomes steeper at high energies. The total incident energy calculated under the assumption that the measured flux at 15 g/cm² consists of primaries is two times greater than the total incident energy appearing as atmospheric ionization.

The east-west asymmetry values reach a maximum of 0.53 ± 0.05 at the equator and decrease to 0.24 ± 0.09 at 40° geomagnetic latitude. The asymmetry to be expected from the latitude effect if all primaries are positive, reaches 1.20 at the equator, and at all latitudes and zenith angles is considerably higher than the observed asymmetry. It is not possible to decide on the basis of the present experiments whether this discrepancy arises from atmospheric effects or from a sizable fraction of negative primaries.

I. INTRODUCTION

A MEASUREMENT of the azimuthal distribution of the primary cosmic radiation at latitudes near the geomagnetic equator, combined with measurement of the vertical flux over a range of latitudes, in principle enables one to evaluate the energy spectrum and to determine the sign of the charge of the primary radiation over a range of energies from about 1 to at least 14 Bev. The majority of the experiments on which our knowledge of the geomagnetic behavior of cosmic rays is based deal almost entirely with secondary cosmic rays generated in the atmosphere. To compare these data with the extensive theoretical calculations of the motion of primary rays which have reached the earth from infinity one must make assumptions which are difficult to test experimentally.¹ It has become apparent that the magnitude of the various geomagnetic effects increases as the observations are extended to smaller depths in the atmosphere, and for some time it has been considered highly desirable to make observations at very high altitude where there is some hope of separating primary cosmic rays from the atmospheric effects.

Preliminary experiments² which studied the zenithal and azimuthal dependence and absorbability in lead of the cosmic radiation at about 20 g/cm² atmospheric depth at 56° N. geomagnetic latitude indicated that although secondary radiation developed particularly at large zenith angles, the bulk of this could be

absorbed with lead filters. The primaries and hard secondaries remaining gave an approximately isotropic distribution in zenith and azimuth. One should expect a nearly isotropic distribution of primary flux at this high latitude. Following these preliminary experiments, measurements have been made of the azimuthal asymmetry and latitude effect of the cosmic radiation at various atmospheric depths, but principally between 15 and 25 g/cm², and at geomagnetic latitudes of 0°, 20°, 30°, and 40°. The experiments were conducted from the U.S.S. Norton Sound on a cruise from Port Hueneme, California, to Jarvis Island and return, by arrangement with the ONR and the Chief of Naval Operations. Project "Skyhook" constant-level balloon facilities were provided on the ship by ONR.

II. EXPERIMENTAL METHOD

A. The Counting Telescope

The basic measuring instrument was a threefold Geiger counter coincidence telescope consisting of three 10×10 in. trays of 1 in. diameter counters spaced 50 in. between extremes. This construction represented a considerable improvement in counting rate and angular resolution over the geometry previously employed.² The advantage of such a large telescope for high altitude measurements has been demonstrated by H. V. Neher and his collaborators.³ It is probably relatively less affected by side showers than are small telescopes composed of single counters, and has superior directional properties. The effective or half-angle opening of this telescope was 11° on a side and 16° on a diagonal of the end section. The area-solid angle product was computed from the geometry, and to a sufficiently good approximation is given by the equation

$$B = (a^2b^2/l^2)[1 - (a^2 + b^2)/3l^2] \quad (1)$$

³ Biehl, Montgomery, Neher, Pickering and Roesch, *Rev. Mod. Phys.* **20**, 353 (1948).

* This work has been assisted by the joint program of the ONR and AEC.

** Now at the University of Minnesota.

¹ See, for example, D. J. X. Montgomery, *Cosmic Ray Physics* (Princeton University Press, Princeton, New Jersey, 1949), for a survey of the literature and discussion of experiments on this subject up to 1948.

² Stroud, Schenck and Winckler, *Phys. Rev.* **76**, 1005 (1949); J. R. Winckler and W. G. Stroud, *Phys. Rev.* **76**, 1012 (1949). The interpretation of these experiments was partially based on some calculations of the angular distribution of primary and secondary particles in the atmosphere. These calculations are unsatisfactory in several respects and are being revised.

assuming an isotropic flux of incident particles at high altitude over the aperture of the telescope, and by

$$B = (a^2b^2/l^2)[1 - (a^2 + b^2)/2l^2] \quad (2)$$

assuming a $\cos^2\theta$ dependence of the incident particle flux on zenith angle θ at sea level. Here a and b are the tray dimensions and l is the separation. Equation (2) is the same up to the second degree terms in a/l and b/l in the brackets as that used by Montgomery⁴ for a similar telescope. The effective area of the end trays is increased about 2 percent by the circular end sections of the counters. The counter tubes were placed side by side in the trays, and a correction must therefore be made for the dead space introduced by the counter walls. The area-solid angle product was first computed neglecting this dead space, and was then multiplied by the factor $(A'/A)^3$, where A is the tray area and A' is the sensitive area of the counters, thus treating the dead space as a kind of inefficiency. The construction of the counter tubes was as described previously² but modified to 10 in. length (9.75 in. effective measured) and with ethylene as a temperature insensitive quenching vapor substituted for ethyl alcohol. The ten counters in each tray were paralleled, with a 10,000 ohm common load resistance and 100 $\mu\text{mf.}$ coupling capacitor to the coincidence circuit. The operating voltage was 1130, about 80 volts above starting. Each tray was provided with an amplifier-clipper stage, a pulse-inverter-sharpener and a Rossi tube. The coincidence output pulse was lengthened into a square wave of 10 msec. suitable for telemetering requirements by an output tube which regenerated back through the screens of the Rossi tubes to form a univibrator circuit. Type 1L4 miniature pentodes were used throughout, and are advantageous because of their high mutual conductance. The resolving time as measured by the accidental rate with a radium source nearby, as well as by observation of the pulse in the circuit was 2 $\mu\text{sec.}$ The corrections to the data due to dead time of the counters and accidentals were negligible. The telescope, complete with high and low voltage dry batteries for 15 hours operation, was an independent unit and was mounted on a horizontal shaft through its center of gravity. In most experiments the bottom counter tray was covered by a 10 \times 10 in. \times 3 cm thick lead plate very close to the counters. This telescope unit was hung by its shaft in a vertical frame (see Fig. 1) with a motor and gear drive arranged to control the zenith position during flight according to a prescribed schedule.

B. Azimuthal and Zenith Mechanism

During flight the entire gondola was rotated with a period of about 18 min. by a large gear and motor about a ball-bearing vertical shaft. This shaft was effectively

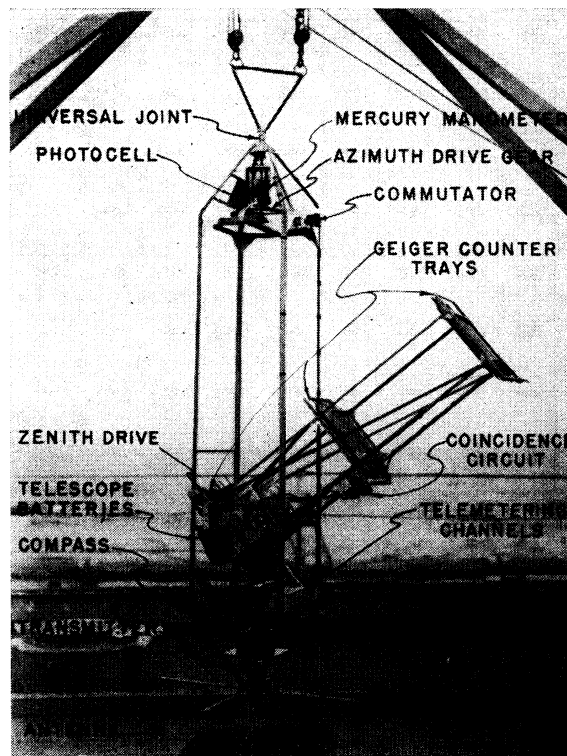


FIG. 1. Complete gondola ready for launching, except for final wrapping.

anchored to the balloon by a non-twisting, double suspension about 10 feet below the balloon load ring.

The azimuthal bearing was determined by a 3 in. nautical compass floating in a 50 percent water-alcohol mixture in a glass cylinder. A light source in the center of the compass housing and four slits in black paper at 90° intervals around the glass housing covered by type 921 photo-tubes constituted the sensing device. A 135° sector secured around the outer edge of the compass float with a height sufficient to block the light beam from the photo-tubes registered a new combination of the four photo-tube signals every 45° of azimuth. The readings were checked in the laboratory by rotating the gondola over an azimuth circle, and during flight the absolute direction of the equipment was determined by a photo-cell recording the sun through a slit. During many of the flights the zenith angle of the telescope was changed periodically from the vertical to 20°, 40° or 60° by a control switch on the azimuth gear and a series of positioning switches which also supplied identification signals for the telemetering system. On some flights the zenith survey was delayed until the balloon reached its ceiling, and during the rising portion the telescope was kept at a fixed zenith position. On a number of flights the zenith mechanism was dispensed with, and the telescope secured at a fixed zenith throughout the flight in the interest of better statistical accuracy.

⁴ R. A. Montgomery, Phys. Rev. **75**, 1407 (1949).

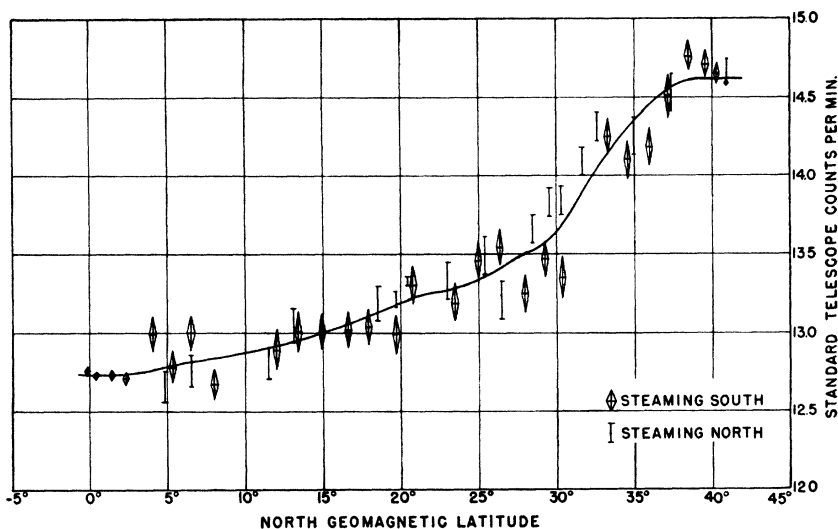


FIG. 2. Latitude effect observed at sea level. Absolute values may be obtained by reference to Table I. Corrected for barometer only.

C. Pressure and Temperature

The pressure was measured during the rising portion of the flight by a "Baroswitch" aneroid element, supplemented by a non-spillable mercury manometer with contacts registering approximately at 8, 10, 12, and 15 mm which spans the pressure range in which the balloon normally levels off. Temperatures were measured by thermistor elements, and remained in a satisfactory range.

D. Telemetry

The telemetry system described previously² was incorporated into the present experiment, but with a

TABLE I. Coincidence telescope constants and flight notes.

Gondola no.	Sensitivity factor*	Flight no.	Date flown	Geomagnetic latitude	Ceiling pressure (g/cm ²)
1	1.013±0.009	2	July 10	0°	15
2	1.008±0.006	5	July 15	0°	31
3	1.038±0.009	6	July 17	0°	19
4	1.012±0.008	7	July 19	0°	24
5	1.023±0.006	3	July 12	0°	13
6	—	4	July 14	0°	—
7	1.031±0.006	8	July 21	0°	20
8	1.000±0.008	9	July 22	0°	—
9	1.028±0.008	10	July 25	20°	16
10	1.003±0.01	13	Aug. 6	20°	15
11	1.012±0.005	12	July 28	20°	13.5
12	1.026±0.006	11	July 27	20°	18
13	1.003±0.004	14	Aug. 10	30°	—
14	1.017±0.005	16	Aug. 14	40°	12
15	1.013±0.005	17	Aug. 15	40°	17
16	0.999±0.01	1	July 3	39°	16
17	0.990±0.0024	15	Aug. 12	31°	13

* Multiply observed counting rate by sensitivity factor to achieve standard telescope rate.

Standard telescope rate at sea level, 40° N. Geo. Lat. = 14.61±0.03 c/min. (Corrected for barometer but not for side showers and absorption in roof and counter walls.) Average of three units. 30 June-3 July and 13 Aug.-15 Aug., 1949.

Standard telescope solid angle = 21.3 steradian-cm², cos²θ distribution. Standard telescope solid angle = 21.6 steradian-cm², isotropic distribution.

$$\text{Flux} = \text{counts/min.} \times \frac{\text{sensitivity factor}}{\text{standard telescope solid angle}}$$

major improvement brought about by adopting an audio F.M. sub-carrier system of transmission. Two sub-carriers were used, one at 7000 cycles/sec. for transmitting the cosmic-ray coincidences, and one at 5400 cycles/sec. which was multiplexed by a mechanical commutator among all the other instruments in the gondola. This multiplexing system including the recorder was identical with that used in the preliminary experiments but was applied to the sub-carrier instead of to the radiofrequency carrier itself. The use of the sub-carrier method resulted in an improvement in stability, signal-to-noise ratio and over-all performance. The use of a separate sub-carrier for the coincidence circuits made it unnecessary to "store" counts pending survey by the commutator, and much higher counting rates could be accommodated without loss.

Details of the sub-carrier system as applied to cosmic ray research will be found elsewhere.⁵ The radiofrequency system was the same as that used previously. All data were recorded on 35 mm film traveling at 6" per minute, the multiplexed portion exactly as before, but a separate 2" cathode-ray tube being photographed for the coincidence impulses. These were recorded singly, every sixteenth pulse being increased in size by a scalar. Also, 0.25 sec. timing impulses were recorded in addition to the 0.2 min. marks used formerly. The complete gondolas ready to fly weighed from 105 to 115 pounds.

E. Standardization Procedures and Sea Level Flux Data

Three telescopes of exactly the same dimension as the gondola units were operated continuously in the vertical position in a light-roofed shelter on the rear deck of the "Norton Sound." In addition to measuring the sea level flux, they were compared with three gondolas at a

⁵ T. Coor, Thesis, Princeton (1948).

time to obtain relative response values. As the construction of the telescopes was closely the same, their counting rates differed by only one or two percent, hardly more than the statistical errors. The mechanical registers in the recording circuits were photographed hourly, and in addition, were read twice daily. In Table I are given numerical data which enable one to convert the counting rate of a given telescope into absolute terms of particles/cm²/sec./steradian. All calibration runs were made without the lead filters. The sea level flux obtained at 40° N. geomagnetic latitude, corrected for barometer but not for side showers and absorption in counter walls, etc., is 0.69±0.01 particles/cm²/min./steradian. Montgomery⁴ obtains 0.695 particles/cm²/min./steradian under similar conditions. Figure 2 presents all the data taken with the standard telescopes

at sea level between 0° and 40° geomagnetic. The total observed effect is 14 percent, which of course includes both the temperature and geomagnetic factors.

The records of the Carnegie Institution cosmic-ray meters at Cheltenham, Maryland, and Huancayo, Peru, were examined^{5a} over July and August. The only noticeable disturbance was a 2 percent decrease at both stations on August 4 coinciding with a magnetic disturbance. The intensity steadily increased to normal in about a week. No flights were made on August 3 or 4, and a flight on August 6 failed to show any difference of the vertical intensity at 15 g/cm² from that of a flight on July 29, both being at λ=20°.

F. Operational Details

Following standardization, gondolas were prepared for flight by following a series of instrument and voltage checks. Geiger tubes were individually checked before and after the standardization runs, and failures were rare. Each section of the telescope and gondola was wrapped with black paper and several layers of cellophane. Launchings followed the standard procedure for "Skyhook" balloons.⁶ The construction of the "Norton Sound" was such as to provide a good wind break and sufficient deck launching space. Competent handling of the ship resulted in good wind compensation and smooth launchings with little strain on the equipment. Most of the flights rose at from 700 to 900 ft./min. and leveled off between 90,000 and 100,000 feet altitude. Radio reception was generally good after some initial difficulties had been rectified, and could be relied on to distances of 350 to 400 miles with the balloon at ceiling, which is about the radio horizon. The

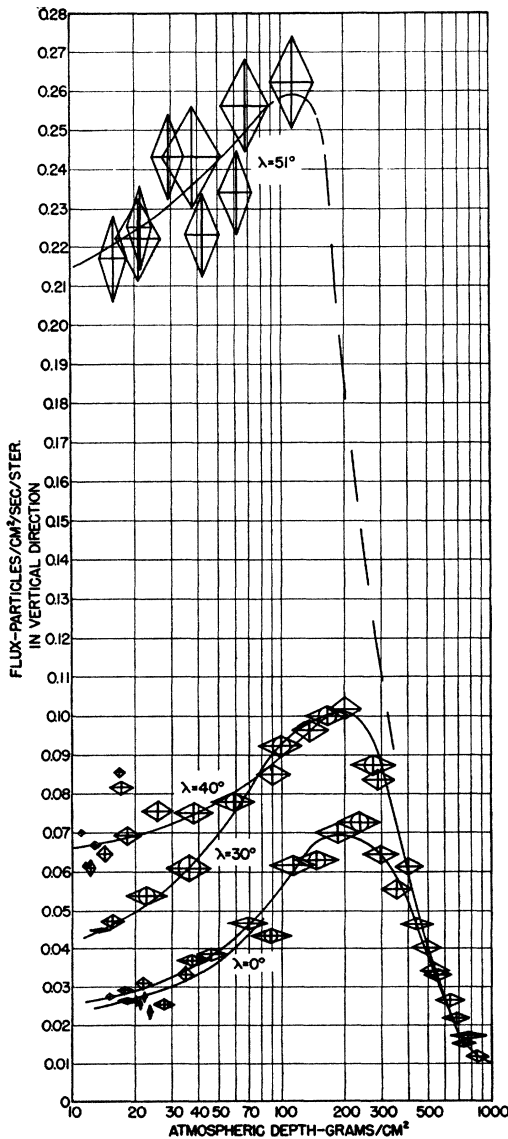


FIG. 3. Vertical flux in the atmosphere at various latitudes, with 3 cm lead filter.

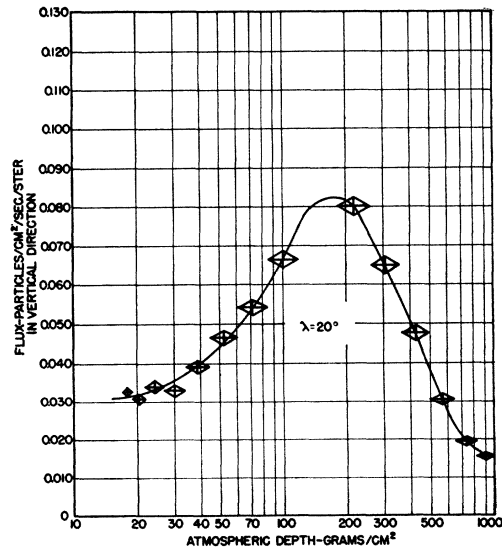


FIG. 4. Vertical flux in the atmosphere at λ=20°, with 3 cm lead filter.

^{5a} Through the kindness of Dr. S. E. Forbush.

⁶ Spilhaus, Schneider, and Moore, J. Meteorology 5, 130 (1948).

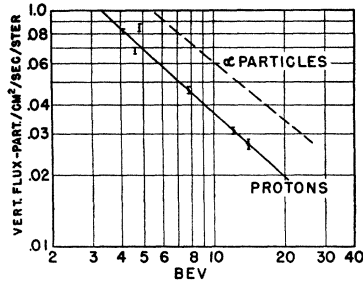


Fig. 5. The integral number-energy spectrum determined from flux measurements at 15 g/cm^2 from $\lambda=0^\circ$ to $\lambda=40^\circ$.

signal passed through two total null points of about 10 minutes duration before the final fade-out on each flight as the balloon drifted away, due presumably to interference between the direct and reflected signals from the sea. None of the gondolas were recovered, so that post-flight checks were not possible. Radar tracking facilities available on the "Norton Sound" provided time-altitude curves and geographic course charts of the balloons within a 75 mile radius of the ship.

G. Shower Detection Experiment

On one flight at 40°N , an attempt was made to measure the effect of bursts or other multiple events on the telescope coincidence rate. Three out-of-line 10 in. counters with about 2 in. spacing between centers were placed just below the center tray of the telescope, and

TABLE II. Flux values at top of atmosphere.

Geom. lat.	Flux particles/cm ² /sec./sterad.	Remarks
0	0.026 ± 0.001^a	Separate flights
0	0.027 ± 0.001	3 cm Pb
0	0.031 ± 0.001^a	No Pb
0	0.028 ± 0.004^b	No Pb
20	0.031 ± 0.001^a	Separate flights
20	0.031 ± 0.001^a	3 cm Pb
28	0.046 ± 0.001^c	18 cm Pb
31	0.046 ± 0.0015^a	3 cm Pb
38.8	0.085 ± 0.003^a	3 cm Pb
39.5	0.068 ± 0.002^a	3 cm Pb
41	0.082 ± 0.002^a	3 cm Pb
41	0.073 ± 0.006^d	No Pb
50	$0.15 \pm ?^e$	Total radiation estimated
50	0.18 ± 0.02^b	No Pb
51	0.22 ± 0.01^f	1.9 cm Pb
52	0.17 ± 0.004^g	0 to 7.5 cm Pb
56	0.23 ± 0.01^h	1.9 cm Pb
58	0.29 ± 0.03^b	No Pb
69	$0.25 \pm ?^i$	Total

^a Winckler, Stix, Dwight, and Sabin, (W, S, D, S)

^b J. A. Van Allen and S. F. Singer, Phys. Rev. **78**, 819 (1950). (U, S)

^c Schein (unpublished). (S)

^d See reference b (G, J, V on figure).

^e D. J. X. Montgomery, *Cosmic Ray Physics* (Princeton University Press, Princeton, New Jersey, 1949), p. 131. (M)

^f J. R. Winckler and W. G. Stroud (unpublished). (W, S)

^g M. A. Pomerantz, Phys. Rev. **75**, 1721 (1949). (P)

^h Winckler, Stroud, and Shanley, Phys. Rev. **76**, 1012 (1949). (W, S)

ⁱ M. A. Pomerantz and M. S. Vallarta, Phys. Rev. **76**, 1889 (1949). (P)

connected to a threefold coincidence circuit which recorded via the multiplexing circuits. The shower counters were parallel to those in the tray, and two of the three were aligned with the telescope axis. This arrangement was designed to pick up bursts coming up from the lead shield over the bottom tray and which might record as a coincidence. Coincidences between the telescope and shower detector could be formed on the film with a resolving time of about 0.2 sec.

H. Analysis of Records

Film reading was greatly facilitated by a motor-driven projector and phototube pick-ups on the observation screen. The 0.25 sec. timing pulses were detected by one photo-tube and recorded by means of a scaling circuit and mechanical register. A similar system was used for the cosmic-ray counts. The flight records were broken down into ten-minute intervals, and in each interval the counts and time were summed in the eight 45° azimuth sectors as indicated by the compass signals recorded in the film.

III. VERTICAL FLUX DATA

Graphs of vertical flux vs. atmospheric depth at various geomagnetic latitudes are shown in Figs. 3 and 4. These data were obtained with the 3 cm Pb filter, and are plotted with pressures on a logarithmic scale to accentuate the region of low atmospheric depths. This scale is approximately linear in height above ground. The vertical extension of the plotted points represents the standard statistical deviation, and the width the pressure range over which the data were averaged. Two flights at $\lambda=0^\circ$ agree quite well (Fig. 3). A vertical flux value at ceiling ($Y=15 \text{ g/cm}^2$ atmospheric depth), was obtained without the lead filter, and gives a slightly higher value (0.032 particles/cm²/sec./sterad.). At $\lambda=20^\circ$ one complete curve was obtained (Fig. 4) with a check point at ceiling from another flight which agrees well. At $\lambda=30^\circ$ one complete curve was obtained. One of the three standard telescope units was used for this experiment, having been equipped with telemetering gear and a lead filter in the field (Fig. 3). At $\lambda=40^\circ$ one complete curve was measured (Fig. 3) with two check points at ceiling. The full curve does not follow the trend established by the $\lambda=0^\circ$, 20° and 30° curves, and fails to show an increased intensity over the 30° latitude at most atmospheric depths. However, at ceiling it levels off at a higher flux value than the $\lambda=30^\circ$ curve. At $\lambda=40^\circ$ there is some scattering of the points at ceiling, and check values obtained on two other flights at ceiling are higher than the full curve. Most of the scattering can be resolved by correcting for the drift of the balloon during flight, or between flights, as the flux increases rapidly with latitude at 40° N . geomagnetic. There remains at $\lambda=40^\circ$ a difference between a point at ceiling obtained on flight No. 1 (July 3) and values on two other flights (16 and 17,

August 14 and 15) which is outside the statistical error. Fluctuations in primary intensity may account for some of these irregularities. Also given in Fig. 3 are some data obtained in Princeton in November, 1948, at $\lambda=51^\circ$ with a small counter telescope of the type used previously.² Between 51° and 56° N. no difference in intensity outside experimental uncertainties at low atmospheric depths was detected with these small telescopes. The $\lambda=51^\circ$ flight carried a 1.9 cm Pb filter. At $\lambda=56^\circ$ various thicknesses between 0 and 17 cm were used, and an appropriate value was chosen for comparison with the $\lambda=51^\circ$ data.

Since all of the flights reached or approached the 15 g/cm² level, the latitude effect can be studied at this depth with little or no extrapolation. In relating the measured values to the flux of primary particles arriving from infinity one is obliged to consider a number of factors, of which the following are important: (A) It is believed that most of the primary cosmic rays interact with the atmosphere with a mean free path between 70 and 150 g/cm² of air. According to this, between 10 and 20 percent of the primaries would have interacted above the apparatus. This fraction will depend strongly on the proportion of heavy nuclei, which seem to have a smaller mean free path.⁷

(B) Experiments show that at this atmospheric depth the vertical flux is nearly all of penetrating nature,^{2,8} at least for $\lambda < 51^\circ$. (C) If the primary interaction produces mesons by the $P-\pi-\mu$ process, the primaries at 15 g/cm² depth should be accompanied by π and μ mesons. We should expect also knock-on nucleons and "satellite" fragments resulting from the break-up of heavy nuclei present in the primary radiation.⁷ These particles together could account for the penetrating flux of (B).

(D) The flux of particles able to penetrate 3 cm of Pb increases with atmospheric depth at small depths and at latitudes between 0° and 40° geomagnetic. There is evidence that at higher latitudes the average penetrability of secondaries decreases.^{2,7} The curves of Figs. 3 and 4 level off with decreasing depth but have obviously not quite reached the plateau above the atmosphere. The single Geiger counter measurements made in rockets exhibit such a plateau⁹ but are not directly comparable with the present experiments. The observed increase with depth indicates that the secondary flux able to penetrate 3 cm Pb builds up faster than the primaries disappear. It is possible that the observed flux is 30 to 40 percent above the flux on the plateau outside of the atmosphere which would have been obtained *with the same equipment*. However, the good agreement between the present results and rocket flux values at 0° and 41° indicates that the effect is

TABLE III. Primary energy flux measured by ionization chambers and counters.

Geom. lat.	(Bev/cm ² /sec.)	
	Millikan <i>et al.</i> ionization chambers	Flux at the "top of atmosphere"
0°		2.16
3°	0.94	
20°		2.25
38°	1.82	
40°		3.40

probably less than the 30 to 40 percent figure, even considering differences in the two kinds of experiments.*

(E) Various geometrical factors, such as secondary particles arriving within the solid angle of the telescope originating from primaries far outside this angle, and air showers able to register a coincidence and coming from far outside the telescope angle must be considered. The asymmetry measurements give an approximate upper limit to such effects of about 20 percent. Part of the increased flux with depth mentioned in (D) may be due to side showers. (F) Particles ejected from the atmosphere in a region of bound orbits may travel above the atmosphere for considerable distances before returning. Qualitative considerations show that the effect would not be important in the vertical direction, but that it might be important at large zenith angles.

We make the assumption that the observed vertical flux at 15 g/cm² is a direct measure of the vertical

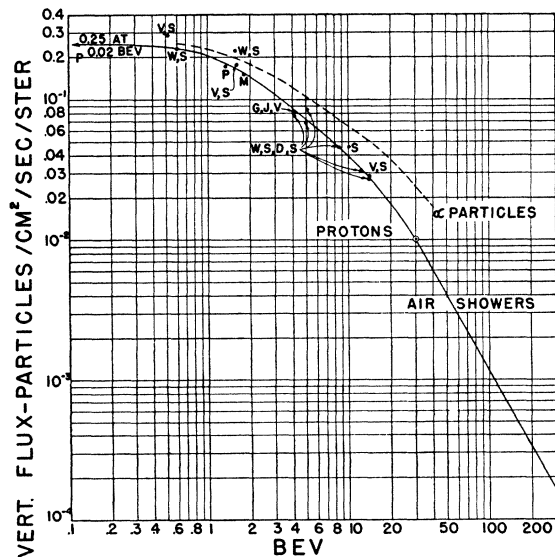


FIG. 6. Integral number-energy spectrum from flux measurements by various investigators at very high altitude. The spectrum given by Hilberry for air showers with $\gamma=2.7$ is joined to form a continuous curve.

⁷ Freier, Lofgren, Ney, and Oppenheimer, Phys. Rev. 74, 1818 (1948); H. L. Bradt and B. Peters, Phys. Rev. 77, 54 (1950).

⁸ M. A. Pomerantz, Phys. Rev. 75, 69 (1949).

⁹ Gangnes, Jenkins, and Van Allen, Phys. Rev. 75, 57 (1949).

* Note added in proof:—Recent rocket measurements (J. A. Van Allen, private communication) with vertical telescopes show that the plateau above the atmosphere is reached as low as 30 km, which is appreciably lower than the beginning of the single counter plateau.

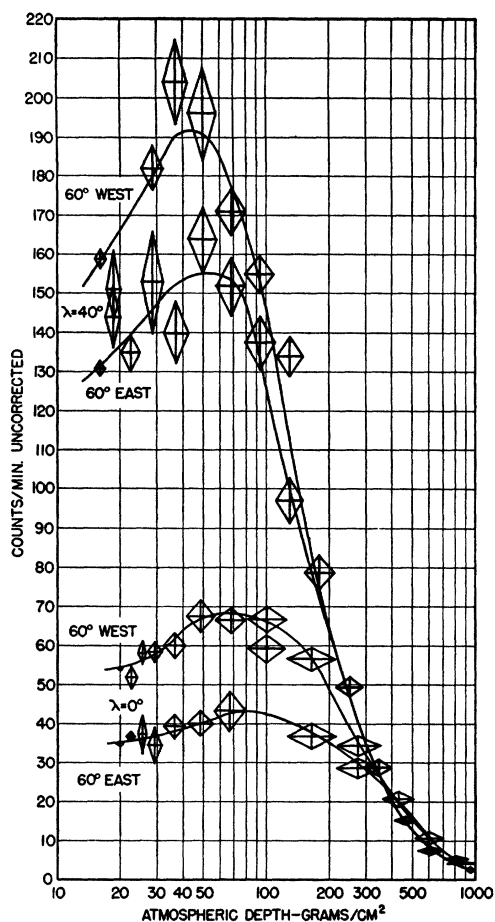


FIG. 7. The eastern and western rates as a function of atmospheric depth at a 60° zenith angle. Data summed in 135° sectors. Upper-gondola 15. Lower-gondola 7. $\lambda=0^\circ$ and 40° .

primary flux, since it is undoubtedly composed largely of primaries, and since the other contributing effects outlined above are probably proportional to the average primary flux. We assume for the vertical cut-off energy that given by the main allowed cone¹⁰ at 0° and 20° . At 30° the penumbra region between the main cone and shadow cone is fairly wide in energy and partially "light," and the cut-off energy is somewhat uncertain. At latitudes of 40° and higher the Störmer cone is used to obtain the vertical cut-off energy. The vertical energy cut-off is independent of the sign of the primaries. The eight measurements of the present experiment, which constitute a self-consistent set all made with identical apparatus, are plotted logarithmically in Fig. 5. A straight line drawn through these points can be represented by the equation $I(E) = 0.30E^{-0.90 \pm 0.05}$ and is the integral number-energy spectrum for primaries, with reservations as discussed above. The differential number-energy spectrum derived from this, i.e., the flux of particles in unit energy interval at E , is $N(E) = 0.27E^{-1.90}$. Over this range of energies primaries

¹⁰ M. S. Vallarta, Phys. Rev. **50**, 493 (1936).

composed entirely of alpha-particles give for the integral spectrum $I(E) = 0.39E^{-0.81}$, and for the differential spectrum $N(E) = 0.32E^{-1.81}$.

In Table II are collected all available flux values obtained at the "top" of the atmosphere and with rockets. These are without exception made with Geiger tube telescopes, but with various geometrical arrangements and amounts of filtering. The best fit to these data plotted in logarithmic form (Fig. 6) appears not to be a straight line, but a curve with increasing slope at higher energies. The agreement between the present

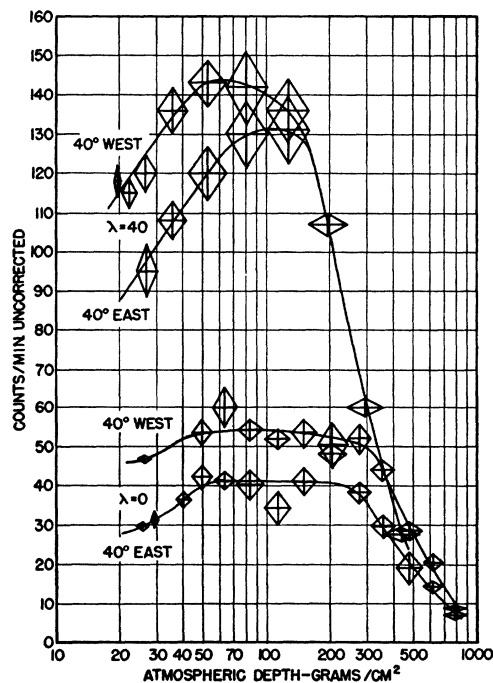


FIG. 8. Eastern and western rates in 135° sectors of azimuth at a 40° zenith angle. Upper-gondola 16. Lower-gondola 4. $\lambda=0^\circ$ and 40° .

experiments and rocket data above the atmosphere at 0° , 41° , and 50° , is noteworthy. The extensive shower spectrum given by Hilberry¹¹ has been drawn in, principally to demonstrate that there is not necessarily a contradiction between the two spectra although the exponents differ by unity, but that they may be joined smoothly. There appears to be a disagreement in absolute value, for according to Hilberry's spectrum $N(E) = 5.45 \cdot 10^{15} \cdot E^{-2.75}$ particles/cm²/sec./ster. which gives $I(10 \text{ Bev}) = 0.01$ particles/cm²/sec./ster. instead of 0.027 as observed here. However, Hilberry's results apply in the region 5.10^{13} to 5.10^{15} ev, and one extends them to 10^{10} ev with considerable uncertainty. The large extrapolation of Hilberry's spectrum to the geomagnetic region of energies below 60 Bev makes the derived flux value in this region very sensitive to the exponent, γ , and the two spectra may be easily brought

¹¹ N. Hilberry, Phys. Rev. **60**, 7 (1941).

into agreement in absolute value by modifying γ by a few percent, or probably by less than the accuracy of Hilberry's result.

From the curve (Fig. 6) it appears that the spectrum levels off at the low energy end (Pomerantz' measurement at $\lambda=69^\circ$), with a rather broad knee between 50° and 60° N. geomagnetic, or definitely further north than the well-known knee at sea level, which occurs at about 45° . One would expect the sea level knee to be south of the high altitude knee because of energy loss in the atmosphere. It is also possible that the high altitude knee measured at 15 g/cm^2 depth is partly attributable to atmospheric absorption. It is known that the ionization range for low energy heavy nuclei which may enter at 56° or higher, may be of this order in g/cm^2 , and depending on the relative abundances of heavies and protons, and their spectra, the exact atmospheric depth may be important at high latitudes even at very high altitudes. It would be very desirable to make a self-consistent set of measurements over the knee region to determine its exact shape and location, as the present points scatter too severely.

It is of great importance to compare the present measurements with the ionization-depth measurements of Millikan, Neher and their collaborators on which a major part of our knowledge of the geomagnetic effects

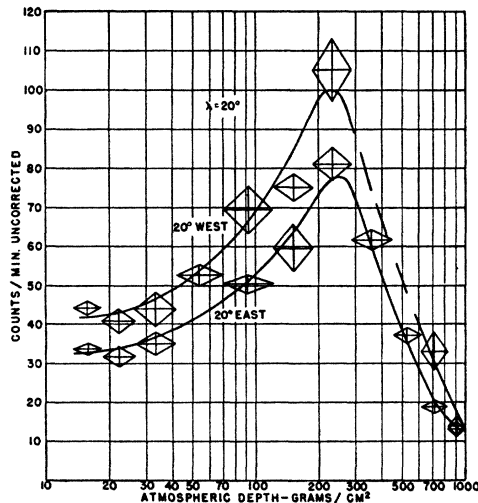


FIG. 9. Eastern and western rates at $\lambda=20^\circ$, zenith angle= 20° . Gondola 11.

is based. To make this comparison we calculate the total incident energy assuming that our observed spectrum holds for energies between 3.5 and 60 Bev for protons, which includes all the geomagnetically influenced proton primaries between 0° and 40° latitude. The Hilberry spectrum was assumed above 60 Bev. This energy flux in $\text{Bev/cm}^2/\text{sec}$. is

$$\Phi(E, \lambda) = \int_{E_{\min}(\lambda)}^{\infty} \Omega(E, \lambda) N(E) E dE. \quad (3)$$

Here $\Omega(E, \lambda)$ is the solid angle of the allowed cone for energy E at latitude λ , and $N(E)$ is the observed differential number-energy spectrum. We derive Ω graphically from the main cone (Vallarta¹⁰) at $\lambda=0^\circ$ and $\lambda=20^\circ$, and from the Störmer and the shadow cones¹² at $\lambda=40^\circ$ from the relation

$$\Omega(E, \lambda) = \int_{\theta_{\min}(E, \lambda)}^{\pi/2} \phi \cdot \sin\theta \cos\theta d\theta, \quad (4)$$

where ϕ is the azimuthal extent of the allowed cone at zenith angle θ . Equation (3) has been integrated graphically and is compared with the Millikan-Neher-Pickering results¹³ in Table III.

The flux measurements give about twice the incident energy appearing as ionization at both low and high latitudes. We expect the measured *flux* values to be high due to multiplication, etc. in the atmosphere, as discussed previously. But this may well be compensated by our calculation of the *energy*, which is performed on the basis of protons alone. Since it is very likely that a 20 to 25 percent α -particle component, as well as much smaller but appreciable numbers of heavier nuclei exist throughout the primary spectrum,^{13a} the effective energy cut-off and the total energy flux would be *higher* at each latitude than the calculated values. The energy calculations based on particle flux measurements are indirect in the sense that the theory of the allowed cone is utilized with no independent check on its accuracy or applicability, a factor which is not present in the ionization measurements. It presumably would be possible by invoking a sufficient particle flux moving in

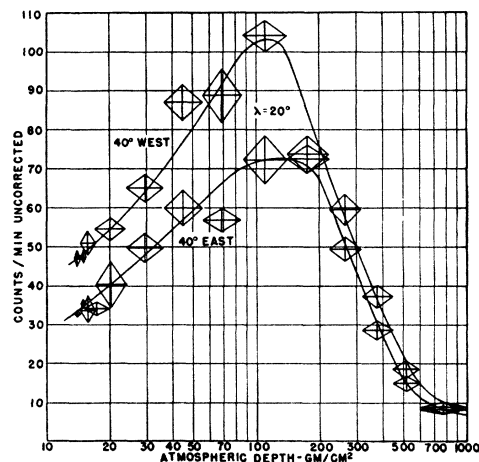


FIG. 10. Eastern and western rates at $\lambda=20^\circ$, zenith angle= 40° . Gondola 10.

¹² E. J. Shremp, Phys. Rev. 54, 153, 158 (1938).

¹³ Millikan, Neher and Pickering, Phys. Rev. 61, 397 (1942). Quoted in L. Jánossy, *Cosmic Rays* (Oxford University Press, London, 1948), p. 298.

^{13a} This fact is established over a part of the primary energy spectrum, and the ratio of alpha's to protons seems not to vary rapidly with energy. (Reference 7, and recent unpublished cloud chamber results of E. P. Ney.)

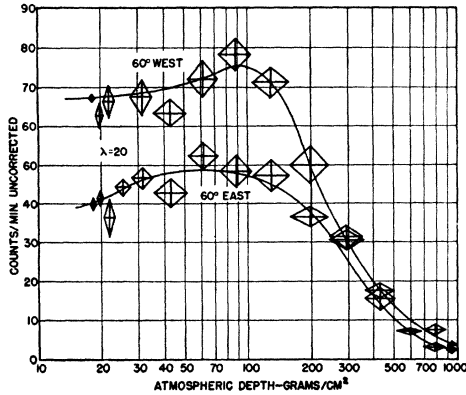


Fig. 11. Eastern and western rates at $\lambda=20^\circ$, zenith angle $=60^\circ$. Gondola 12.

bound orbits, which have not been studied theoretically so far, or by assuming that the equivalent magnetic dipole field of the earth at large distances from the earth is not given by the distribution of magnetic flux on the surface, to explain part of all of the observed differences. However, the large discrepancy shown in Table III can be accounted for most reasonably by primary energy passing into forms not detectable by the ion chambers, such as neutrinos, low energy nuclear fragments and binding energy absorbed during nuclear evaporations of air atoms.

Jánossy (reference 13, pp. 299–300) finds that the Millikan ionization data as well as the vertical energy flow measured with counter telescopes¹⁴ can be accounted for in terms of a differential number-momentum spectrum of the form $c \cdot p^{-\gamma}$ with $\gamma=2.5$. The higher value of γ obtained from such measurements made lower in the atmosphere is related to the difference in absolute energy flux shown in Table III. If, as suggested above, these differences are due to non-ionizing forms of secondary radiation such as neutrinos, then Table III suggests that the relative fraction going into neutrinos must be higher for higher energy primaries (lower latitudes).

IV. AZIMUTHAL DATA

The azimuthal effect was studied as a function of atmospheric depth by collecting the data in three 45° western and eastern sectors. The result of averaging the telescope counting rate over 135° of azimuth in each direction was to decrease the observed E–W asymmetry, but was necessitated by the short time spent by the balloon in each pressure interval during the ascent of the flight. Ten minute intervals were used during most of the ascent, but were increased in length near ceiling as the balloon leveled off, and the lowest pressure points include all of the ceiling data averaged together. In this type of analysis no reference was made to the azimuthal standardization, and the two 135° sectors represent the eastern and western directions only to

¹⁴ Millikan, Neher, and Pickering, Phys. Rev. **63**, 234 (1943).

within 15° or 20° . In one or two of the intervals during ascent the balloon rotated so rapidly that the inertia of the compass produced considerable overshooting and lagging in the azimuthal indications. This effect was discovered by correlating the sun reference photo-cell with the compass, and it was noticed that during such intervals the east-west values fluctuated beyond the statistical error, and usually the east-west asymmetry was reduced. Fortunately, these intervals were not numerous enough to influence the average curve appreciably.

Figures 7 and 8 give the E–W effect as a function of depth for $\lambda=0^\circ$ and $\lambda=40^\circ$, for 40° and 60° zenith angles. Figures 9, 10 and 11 give similar curves at $\lambda=20^\circ$ for 20° , 40° , and 60° zenith angles. These curves show that the E–W effect increases with decreasing depth, and does so with increasing rapidity between 300 and 100 g/cm^2 . The E–W effect is larger at $\lambda=0^\circ$ than at $\lambda=40^\circ$, as would be expected from geomagnetic considerations, and apparently at $\lambda=0^\circ$ persists relatively further into the atmosphere than at $\lambda=40^\circ$. Both the easterly and westerly curves pass through a mild maximum between 50 and 100 g/cm^2 . Above this, at $\lambda=0^\circ$ a leveling off process seems to take place, but at $\lambda=40^\circ$ a sharp downward trend persists to the highest altitudes reached. It was hoped that such data would permit the trend of the asymmetry to be mapped out as

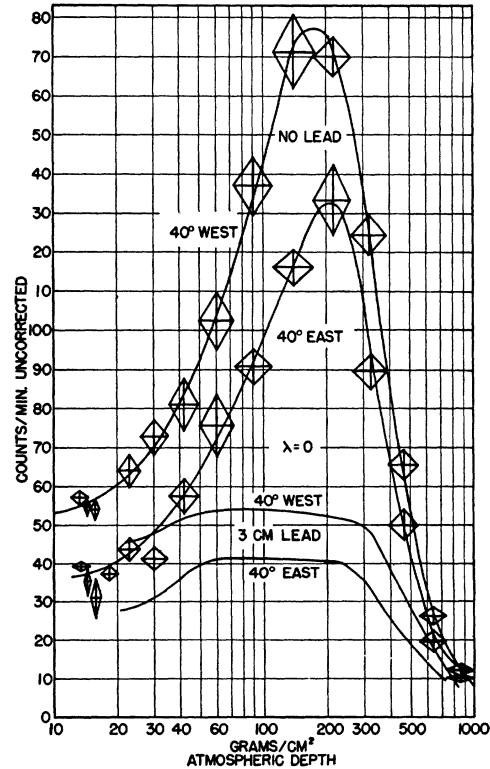


Fig. 12. Eastern and western rates at $\lambda=0^\circ$, zenith angle $=40^\circ$ without the customary 3 cm Pb filter. Lower curves—same measurement with filter.

a function of depth near the top of the atmosphere, as an aid in estimating the effect of the atmosphere on the measurements. However, if the asymmetry is plotted as a function of depth in this region no consistent picture emerges. In some cases the asymmetry remains constant, and in others it increases or decreases. It is probable that the statistical accuracy during the ascending portion of the flights is not sufficient to give detailed information of this sort.

Of more interest is the curve in Fig. 12, at $\lambda=0^\circ$, 40° zenith angle *without* the 3 cm Pb filter. Large maxima occur in both the east and west portions, and the asymmetry, or at least the E-W difference, is preserved to a surprising degree. For comparison the corresponding curve with the 3 cm Pb filter is shown. The asymmetry without the filter is only a little smaller at various depths than with it, a result which is in agreement with measurements made by H. V. Neher and collaborators¹⁵ at 250 to 300 g/cm² atmospheric depth. The asymmetry measured from Fig. 12 between 100 and 200 g/cm² is about 27 percent. The asymmetry at the top of the atmosphere, and with the data summed in 45° sectors, increases to 50 percent without lead, and 54 percent with 3 cm (see Table IV). The trend is obviously towards smaller asymmetries with greater depths, wider sectors of azimuth, and less filtering. It seems possible on the basis of this to explain in most part the low asymmetry measured by Johnson and Barry¹⁶ at

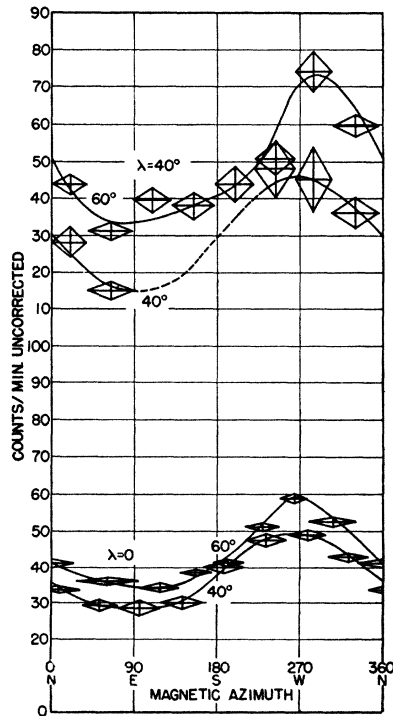


FIG. 13. Azimuthal effect at $\lambda=0^\circ$ and $\lambda=40^\circ$, with zenith angles of 40° and 60° . Gondola numbers top to bottom—15, 15, 7, 4. Atmospheric depth top to bottom—17, 17, 20, 24 g/cm².

¹⁵ Biehl, Neher, and Roesch, Phys. Rev. 76, 914 (1949).

¹⁶ T. H. Johnson and J. G. Barry, Phys. Rev. 56, 219 (1939).

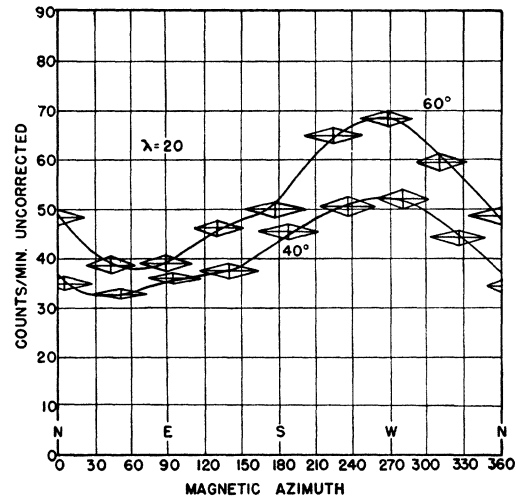


FIG. 14. Azimuthal effect at $\lambda=20^\circ$, zenith angles= 40° and 60° . Gondolas 10 and 12. 15 and 18 g/cm², respectively.

$\lambda=20^\circ$, and at about the 100 g/cm² level at a 60° zenith angle. Their telescope was composed of small counters with about a 90° total opening, and data was summed in the 180° E-W sectors. In the present experiments we note that the 50 percent peak asymmetry is reduced to 32 percent if we average over the two 180° sectors, and the atmospheric depth effect further reduces this to about 20 percent. The difference between this and the 7 ± 3 percent measured by Johnson might be accounted for by less obvious features of the two experiments such as the small single counter telescope *vs.* the large tray construction, measurement of azimuth, etc.

Unfortunately, the low statistical accuracy of the present data at the 250 to 300 g/cm² depth, where the balloon spends little time, makes a direct comparison with the Neher data¹⁵ which has high statistical accuracy, inconclusive.

The azimuthal effect measured at the balloon ceiling where a number of hours of data were collected is shown in Figs. 13, 14 and 15. These data were collected at the number of g/cm² indicated under the figure with an uncertainty of a few g/cm² arising from the averaging process over the balloon's time-altitude curve and the finite pressure increments indicated by the manometer contacts. On most flights the balloon remained within an interval of about 5 g/cm² after reaching maximum altitude, which varied between 15 and 25 g/cm². The number of counts and the time were summed in each azimuthal sector in ten-minute intervals as described in Sec. II-H, and totals and rates in each sector were then obtained for the entire constant level portion of the flight. Reference was made to the exact compass calibrations and the sun reference indicator to determine the angular width and magnetic azimuth of each sector. Magnetic north was assumed to lie in the meridian plane through the point of observation of the off-center

equivalent dipole representing the earth's field.¹⁷ The height of the plotted point is the standard statistical deviation, and the width is the azimuthal extent of the sector. These curves as plotted represent the telescope data uncorrected for variations in balloon altitude on different flights, or for the telescope sensitivity, etc. Absolute flux values may be computed easily with the aid of Table I, but all counting rate curves can be compared directly, due to the similarity of the separate telescopes. The gondola numbers are given under the figures.

Figure 13 gives the measured azimuthal effect at $\lambda=0^\circ$ and $\lambda=40^\circ$ at 40° and 60° zenith angles. We find a much larger flux and smaller percentage asymmetry at $\lambda=40^\circ$ than at $\lambda=0^\circ$, in accordance with theoretical expectations. It is notable that the asymmetry at a 60° angle is inappreciably larger than at a 40° angle, and furthermore, the eastern intensity is larger for 60° than for 40° zenith, which is contrary to the predictions of the theory if all the primaries are positively charged. The azimuthal curves at $\lambda=20^\circ$ carry out these same features (Fig. 14), but in qualitative agreement with the main cone diagram for this latitude, the curves are shifted in phase somewhat from the $\lambda=0^\circ$ curves, and have an additional inflection point at approximately 180° magnetic azimuth. The statistical accuracy of the measurements is not good enough to confirm the existence of a north-south effect as predicted theoretically.

In Fig. 16 is shown a comparison of the azimuthal effect at $\lambda=0^\circ$ at zenith angles of 40° and 60° with and without the 3 cm lead shield. The no-lead experiment yields a slightly larger flux, even though its atmospheric depth is less. The asymmetry, however, is very little different with and without the lead shield. This can be interpreted as evidence that the contribution to the counting rate from large energetic star fragments is small, as a large fraction of such star particles would be absorbed in 33 g/cm² of lead. The familiar isotropic distribution of such fragments would certainly conceal the directional properties of the primaries responsible for

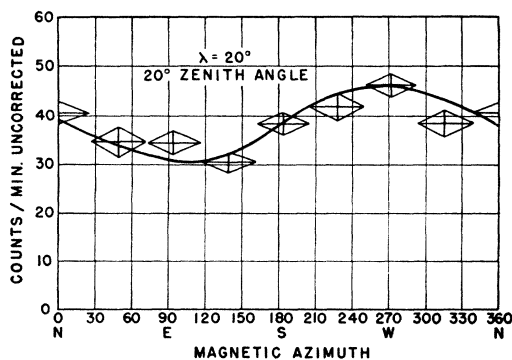


FIG. 15. Azimuthal effect at $\lambda=20^\circ$, zenith angle = 20° . Gondola 11, 13.5 g/cm².

¹⁷ J. Bartles, Terr. Mag. 41, 225 (1936).

TABLE IV. Observed and predicted azimuthal asymmetry.*

Geom. lat.	Zenith angle	E. min. (Störmers)		Predicted asymmetry	Observed asymmetry**
		E.	W.		
0°	40°	0.615	0.430	0.81	0.50±0.08 (No Pb)
	60	0.730	0.420	1.20	0.50±0.09 (No Pb)
	40	0.615	0.430	0.81	0.54±0.10 (3 cm Pb)
	60	0.730	0.420	1.20	0.53±0.05 (3 cm Pb)
20°	20	0.520	0.437	0.41	0.41±0.10 (3 cm Pb)
	40	0.583	0.420	0.71	0.48±0.06 (3 cm Pb)
	60	0.680	0.410	1.08	0.58±0.05 (3 cm Pb)
40°	40	0.317	0.275	0.31	0.24±0.09 (3 cm Pb)
	60	0.500	0.270	1.02	0.26±0.07 (3 cm Pb)

* Asymmetry = $(I_w - I_e) / \frac{1}{2}(I_w + I_e)$.

** Errors determined by calculating the asymmetry with opposite extreme values of I_w and I_e as given by the standard statistical errors in I_w and I_e .

them. Similar remarks apply to other low energy particles produced at wide angles.

Figure 4 of reference 2 shows the absence of an azimuthal effect at $\lambda=56^\circ$ greater than five percent.

The observed east-west asymmetry values obtained from the curves of Figs. 13, 14, 15 and 16 are collected in Table IV. To test the hypothesis that the primary spectrum consists entirely of positive particles the asymmetry is predicted from the latitude effect of the vertical flux which does not depend on the sign of the charge, but only on the energy spectrum. If all primaries are positive, the azimuthal and latitude effects should be identical as long as the minimum energy of entry expressed in Störmers is the same. The range of Störmers covered by the east-west effect is given in column 3 of Table IV. The range covered by the vertical cut-off extends only to 0.500 Störmers, so that some extrapolation of the vertical flux data is necessary to 0.730 Störmers, the eastern minimum energy at 60° zenith and $\lambda=0^\circ$. This type of comparison entirely on the basis of Störmer units and using the observed vertical flux is independent of the e/m ratio of the primaries, and is dependent only on the self-consistency of the theory.

The observed asymmetry is plainly less by a considerable factor than that predicted, with the exception of $\lambda=40^\circ$, $\theta=40^\circ$ and $\lambda=20^\circ$, $\theta=20^\circ$. The factor is much larger than the statistical errors in the asymmetry curves and cannot be accounted for by the various uncertainties in the vertical flux of the type discussed in Sec. III. On the contrary, indications are that the spectrum becomes steeper at higher energies, with γ changing from 1.9 to 2.7, so that the predicted asymmetry might be larger than the calculated value, but certainly not smaller. The azimuthal distribution is probably the most self-consistent of all the measurements, as it is determined with a single instrument repeatedly surveying the complete 360° region, and at quite constant atmospheric depth.

One of the most obvious effects to be studied in explaining the low observed asymmetry is that of the

residual atmospheric path above the equipment, which is longer at zenith angle θ by the factor $\sec. \theta$ than the vertical path. The zenith angle effect at constant minimum energy (and therefore constant primary flux) may be studied by selecting directions intersecting lines of constant Störmer units as given for example in the main cone projections of Vallarta.

In Table V are tabulated the observed counting rates of the telescopes at a number of combinations of the geomagnetic latitude λ , azimuth ϕ and zenith angle θ , which theoretically should correspond to a fixed minimum energy. Two such minimum values, 0.5 and 0.43 Störmers (14 and 10 Bev for protons) are selected, and all positive primaries are assumed. The following points should be noted concerning Table V: (A) The $\theta=0^\circ$ and $\theta=40^\circ$ rates for the same minimum energy are in satisfactory agreement. The $\theta=20^\circ$ values at $\lambda=20^\circ$ are somewhat low, but this measurement may reflect the smaller depth obtained on this flight. These zenith angles do not intersect the chosen minimum energies as far north as $\lambda=40^\circ$. (B) At $\theta=60^\circ$ the rate at $\lambda=0^\circ$ and $\lambda=20^\circ$ is uniformly higher by 15 to 20 percent for equal minimum energies than the smaller zenith angles. (C) At $\lambda=40^\circ$ the $\theta=60^\circ$ rate is higher by a factor of *three* than any of the other rates for equal minimum energy.

From point (A) one can conclude that the difference in air path between the vertical and $\theta=40^\circ$ has a small effect on the measurements at about 15 or 20 g/cm² atmospheric depth, as the rates are nearly the same for the same minimum energy. The longer path at $\theta=60^\circ$ produces a noticeable increase in rate, but if we compare with the vertical data on the basis of equal air path in g/cm² as well as equal minimum energy, very reasonable

TABLE V. Observed rates for fixed minimum energy with λ , θ and ϕ variable.

0.500 Störmers [$E=14$ Bev for protons]								
λ	$\theta=0$		$\theta=20$		$\theta=40$		$\theta=60$	
	ϕ	Rate	ϕ	Rate	ϕ	Rate	ϕ	Rate
0	~	40	88	—	196	41.5	201	45
			351	—	344	39.5	338	46.5
20	—	—	19	37	158	40	170	50
			128	31	352	40	350	51
40	—	—	—	—	—	—	40	137
							115	135
0.430 Störmers [$E=10$ Bev for protons]								
λ	$\theta=0$		$\theta=20$		$\theta=40$		$\theta=60$	
	ϕ	Rate	ϕ	Rate	ϕ	Rate	ϕ	Rate
0	—	—	—	—	—	—	260	59
							280	58
20	—	—	—	—	209	48	201	58.5
					288	51.5	294	65
25	~	47	—	—	—	—	—	—
40	—	—	—	—	—	—	10	146
							130	136

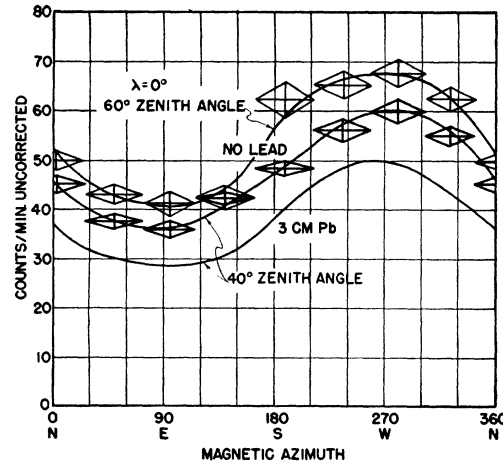


FIG. 16. Azimuthal effect at $\lambda=0^\circ$, zenith angles= 40° and 60° , with and without the 3 cm Pb filter. Top, gondola 5, 13 g/cm². Bottom, gondola 4, 24 g/cm².

agreement between the $\theta=0^\circ$ and $\theta=60^\circ$ data results at latitudes up to 25° . This comparison is made by reading the vertical rate curves at a depth $Y \sec. \theta$, where Y is the balloon depth, and ignores meson decay effects.

The large factor which appears at $\lambda=40^\circ$ is far greater than can be explained by simple air path considerations. We note also that the largest discrepancy between the predicted and observed E-W asymmetry (Table IV) occurs at $\lambda=40^\circ$, $\theta=60^\circ$. The fact that with a simple air path correction the intensities at various zeniths and latitudes for the same minimum energy agree seems at first a contradiction to the data given in Table IV, which indicates *disagreement* of a similar comparison assuming all positive primaries. We note, however, that the data in Table V which agree best (mostly for 0.5 Störmers) lie predominantly in the northerly or southerly directions. In these directions, like the vertical, the intensity depends only to a slight degree on the polarity of the particles. The northern or southern intensity is also near the mean value of the east and west intensities.

Another atmospheric effect is the presence of secondary particles produced or scattered upward toward the east, and originating from primaries arriving from the west. Neher and his collaborators¹⁵ find a negligible amount of upward radiation at 300 g/cm² depth, but this is not surprising since the number of primaries which are moving at large zenith angles below this depth, and which therefore are able to produce upward secondaries into the equipment, is very small. This is not true at the top of the atmosphere, however, where even in the horizontal direction an appreciable number of primaries may be present (the ratio of the horizontal air path to the vertical is 27 due to earth curvature, see reference 2). The amount of such upward radiation which would be necessary to reduce the predicted asymmetries to the observed values can be calculated easily

TABLE VI. Estimate of the effect of upward moving particles on asymmetry values.

Geom. lat.	Zenith angle	Observed eastern rate $I(E)$ c/min.	Eastern rate for agreement $I(E_c)$ c/min.	$\frac{I(E)-I(E_c)}{I(W)}$
$\lambda=0^\circ$	40 (no Pb)	36.0 ± 1.5	25.4	0.18
	40	28.5 ± 2.0	21.0	0.15
	60	34.5 ± 1.5	14.8	0.33
$\lambda=20^\circ$	20	30.5 ± 2.0	Agrees	0.00
	40	32.5 ± 1.0	25.0	0.14
	60	38.0 ± 1.5	20.6	0.25
$\lambda=40^\circ$	40	115 ± 5	108	0.05
	60	135 ± 5	57	0.45

by equating these two values and solving for the easterly counting rate as an unknown. In Table VI is listed at each latitude and zenith angle the observed easterly counting rate, the easterly rate which would produce agreement between the E-W and latitude effects, and the difference expressed as a fraction of the westerly rate at the same zenith angle. The fractions range from 5 to 45 percent, in general being larger for the larger zenith angles. This is of course to be expected since momentum considerations would predict that most energetic secondaries would be projected forward, with few at larger angles to the primary direction. Detailed calculations of the type attempted earlier² involving the primary absorption, and the angular distribution and absorption of secondaries may show if this sort of process can satisfactorily produce the amount of upward radiation required by Table VI. That the observed discrepancy can be accounted for by this process seems likely, and one therefore hesitates to invoke any negative primaries until further work is done. However, the necessary flux of primary electrons is a small enough fraction of the total flux to have escaped observation at high latitudes where direct experiments for detecting primary electrons have been carried out.^{18,19*} The above discrepancy between the E-W and latitude effects apparently does not exist at 300 g/cm², where Neher and his collaborators¹⁵ find agreement between the east-west effect at $\lambda=25^\circ$, $\theta=45^\circ$ and the vertical latitude effect over the interval $\lambda=0^\circ$ to $\lambda=29^\circ$. A similar result is obtained at greater depths, even at sea level.²⁰ However, it is notable that the latitude effect of the vertical flux between $\lambda=50^\circ$ and $\lambda=0^\circ$ is 1.1 at sea level, 1.6 at 300 g/cm² and 6.3 at 15 g/cm². The E-W asymmetry is 0.10, 0.30 to 0.35, and 0.54 at the

¹⁸ R. J. Hulsizer, Phys. Rev. **73**, 1252 (1948).

¹⁹ M. Schein, quoted in D. J. X. Montgomery *Cosmic Ray Physics*. See reference 1.

* *Note in proof*:—A recent analysis of 1625 cloud chamber photographs obtained by E. P. Ney at the top of the atmosphere shows that electrons of 1 Bev or over can not constitute more than 0.2 percent of the primary flux at 56° N Geom. Electrons at low latitudes therefore constitute not more than 2 percent of primaries, and can not explain the present discrepancy. (Critchfield, Ney, and Oleksa, Phys. Rev. **79**, 402 (1950)).

²⁰ T. H. Johnson, Rev. Mod. Phys. **10**, 193 (1938).

same respective depths at the equator, and does not increase enough with decreasing depth to be consistent with the increase of the latitude effect with depth below 300 g/cm², for positive primaries. Directional measurements, like many other types of cosmic ray phenomena, obviously reflect at each point in the atmosphere those primary particles whose energy is great enough to make their effects felt at that point. The weighting effect of the atmosphere on the number-energy distribution of primaries is very pronounced, and thus the measurements at a depth of $\frac{1}{3}$ atmosphere effectively span a different range of primary energies than the "top of the atmosphere" data, even though the latitude and direction in space may be the same. The agreement in one case and lack of agreement in another between the latitude and E-W effects may therefore not be contradictory if the measurements are made at different depths in the atmosphere.

V. SHOWERS AND BURSTS

One experiment at $\lambda=40^\circ$ (Flight 16) was conducted with counter tubes arranged to detect bursts or air showers (see Sec. II for counter arrangement). The main telescope was vertical during ascent, and the multiple events recorded increased, passed through a mild maximum at a somewhat smaller atmospheric depth than the maximum observed with the telescope, and then decreased near the top of the atmosphere. The multiple events were 15.6(c/min.)/125(c/min.) = 13 percent of the telescope rate at maximum, and 13.5(c/min.)/80.5(c/min.) = 17 percent at ceiling (12 g/cm²). There was a marked zenith angle dependence, for the rate with the telescope at $\theta=0^\circ$ was 13.5 ± 0.6 c/min., at $\theta=40^\circ$ was 14.8 ± 0.5 c/min. and at $\theta=60^\circ$ was 16.0 ± 0.5 c/min., averaged over several cycles of the telescope. The corresponding telescope rates averaged in azimuth were respectively 80.5, 92.5 and 104.9 c/min., which gives for the ratio of multiple events to telescope events 0.17, 0.16 and 0.15, which is constant within statistical errors. Coincidences between the shower detector and the main telescope could only be formed on the recorder film with rather poor resolving time (0.2 sec.), but an analysis showed that the measured coincidence rate of from 3 to 6 c/min. could be entirely accounted for by accidentals, and the true coincidence rate was therefore a negligible part of either the shower detector or of the telescope rate. The geometry of the shower detector was such as to favor bursts coming up from the lead shield over the bottom counter tray and which would also pass through the telescope. However, the shower detector undoubtedly discriminates against the bursts of fewer particles, as the solid angle subtended by the shower detector at the lead shield is very small. Furthermore, bursts in which only a single particle escaped up through the telescope would in no case be detected as a shower. Considering that the telescope solid angle for bursts is only 1/25 steradian,

the single particle type might well be most frequently recorded. Better evidence against bursts from the lead shield is the slight increase, rather than decrease in telescope rate with the shield removed at $\lambda=0^\circ$.

Some calculations have been made of the response of the telescope to showers, either of the electron cascade, or multiple-meson type. These calculations predict the probability of registering a shower as a function of the zenith angle and particle density. But since neither the intensity, zenith angle or density distribution of showers is known at the top of the atmosphere, this method of approach is at present unsuccessful.

VI. DISCUSSION AND CONCLUSIONS

The foregoing investigation yields two principal results. The first of these, the number-energy spectrum of primary cosmic rays, is obtained from the vertical flux measurements at various latitudes. The success of this measurement depends on how completely the flux of ionizing particles at about 15 g/cm² matches, in number and direction, the primary flux. The assumption is made that the measured ionizing particles capable of penetrating 3 cm of Pb are largely primaries, and that the remainder of events are proportional to the primary flux. The various measurements can then be satisfactorily represented by the differential number-energy spectrum $N(E) = KE^{-\gamma}$. If the primaries are all assumed to be protons, $K=0.27$ and $\gamma=1.90$. If all α -particles are assumed, $K=0.32$ and $\gamma=1.81$. There is evidence that the true situation is a combination of about 75 \pm 10 percent of protons and 25 \mp 10 percent of α -particles. If the flux at 15 g/cm² has a constant proportionality to the true primary flux at various energies, then the exponent γ is correct. This condition seems to be not too stringent and the differential number-energy spectrum adopted is $N(E) = 0.27E^{-(1.90 \pm 0.05)}$ over the energy range from 1 to at least 14 Bev. It is evident that the present experiments determine γ much better than they do the constant K . The proton spectrum is adopted because then the various atmospheric effects, which if corrected for would apparently reduce the K -value, may be compensated by the α -particle component, which would increase K . The total incident energy calculated from this spectrum, combined with the high energy spectrum obtained from air showers, is twice that appearing as ionization in an atmospheric column as measured by Millikan, a factor of difference which seems well beyond experimental uncertainties. It is suggested

that most of this difference may be due to secondary energy forms which escape the ionization chamber.

The second principal result is obtained by comparing the E-W and latitude effects over the same energy ranges. This can be done independently of the nature of the particles by using Störmer units of energy. In nearly every case the E-W effect is smaller than the latitude effect. It is here suggested that scattering or production of particles upward from below the measuring instrument may account for the differences, and that this effect should be investigated before negative primaries are assumed.

It would be desirable to increase the statistical accuracy of the experiments, but it seems obvious that the possible atmospheric influences are considerably larger than the purely statistical errors. It is regrettable that none of the equipment was recovered for post-flight checks, but a number of other methods of following the behavior of the apparatus indicated that the data presented here have satisfactory reliability. Although the design of the measuring telescope is such as to reduce the effects of air showers and locally produced bursts, the exact influence of these factors is not well-known.

The present investigation appears to contain significant data on the zenith angle effects, and the analysis of these will be given in a later communication.

The authors wish to express their sincere thanks to staff members of the Princeton Naval Ordnance Laboratory and to members of the Princeton faculty, particularly Professors J. A. Wheeler and G. T. Reynolds, for major support of the effort. The successful development of the constant-level plastic balloon by members of the General Mills Aeronautical Research Laboratory made the program feasible. Through the kindness of the ONR and the Chief of Naval Operations arrangements were made for the shipboard operation, and it is a great pleasure to acknowledge the excellent cooperation of the officers and crew of the U.S.S. NORTON SOUND, John Quinn, Captain U.S.N., commanding officer. The construction of special equipment, preparation for flight and modification of the gondolas, and the successful balloon launchings were made possible by the high technical caliber of personnel aboard the NORTON SOUND. The authors were privileged on numerous occasions during the fall of 1949 to discuss the experimental results with Professor M. S. Vallarta of the Institute for Advanced Study, Princeton.

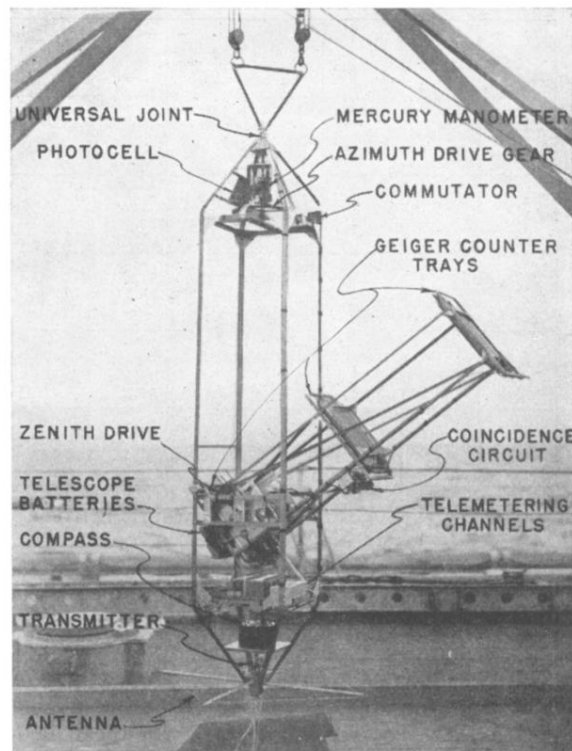


FIG. 1. Complete gondola ready for launching, except for final wrapping.